

Resonance ultrasonic vibrations for crack detection in photovoltaic silicon wafers

W Dallas, O Polupan and S Ostapenko

University of South Florida, Nanomaterials and Nanomanufacturing Research Center,
4202 East Fowler Ave, Tampa, FL 33620, USA

E-mail: ostapenk@eng.usf.edu

Received 10 November 2006, in final form 14 December 2006

Published 5 February 2007

Online at stacks.iop.org/MST/18/852

Abstract

The resonance ultrasonic vibrations (RUV) technique is adapted for non-destructive crack detection in full-size silicon wafers for solar cells. The RUV methodology relies on deviation of the frequency response curve of a wafer, ultrasonically stimulated via vacuum coupled piezoelectric transducer, with a periphery crack versus regular non-cracked wafers as detected by a periphery mounted acoustic probe. Crack detection is illustrated on a set of cast wafers. We performed vibration mode identification on square-shaped production-grade Si wafers and confirmed by finite element analyses. The modelling was accomplished for the different modes of the resonance vibrations of a wafer with a periphery crack to assess the sensitivity of the RUV method relative to crack length and crack location.

Keywords: photovoltaics, crack detection, micro crack, solar cell, defect, wafer, silicon, resonance, acoustics

(Some figures in this article are in colour only in the electronic version)

1. Introduction

During times of increasing energy costs, renewable energy sources are looked to as a means to save energy consumers from a crisis. Solar cells and panels are currently available to provide direct conversion of solar energy into usable electricity, often being connected to power grids for mass distribution. To compete with traditional fossil energy sources, the solar or photovoltaic (PV) industry is driven by economic reasons to make solar panels of the highest power conversion efficiency along with high reliability at the lowest possible production cost. Being the second most abundant material in the earth's crust and one of the most studied elements, crystalline silicon (c-Si) has taken a dominant role in contributing to over 90% of the entire power module production. As an example of the marketplace today, single crystal Si technology offers solar cells with costs of \$3 to \$4 per peak watt of power, at conversion efficiencies in the range of 18 to 20%. For lower quality multicrystalline silicon (mc-Si) solar cells with approximately 16% efficiency the price ranges from \$2.50 to \$3.00 per peak watt. It is important to recognize that the silicon wafer is a large contributor, up

to 75%, to the overall cost of the solar cell. In addition, the silicon raw material price has roughly doubled in the last two years due to a worldwide shortage of the polycrystalline silicon feedstock. To compensate for the feedstock shortage, solar Si wafers are sliced thinner with thicknesses down to 80–200 μm . Wafer areas have also been increased to reduce overall production costs and larger sized, up to 210 mm \times 210 mm square shaped, wafers are now available. These technological trends make wafer handling in production more challenging and reduce the yield of solar cell lines due to increased wafer and cell breakage. In-line wafer breakage also reduces equipment throughput as a result of down time and the need to stop and clean out machinery to remove broken wafers from the fixtures, which is typically a manual process. Wafer breakage during a production procedure can often lock up a whole process for minutes or longer for cleaning up the automatic belt conveyor and possibly cause costly damage of the equipment.

Various c-Si growth methods such as Czochralski, float zone, casting, edge-defined film-fed growth (EFG) and ribbon are in use with goals of minimizing cost while maximizing cell efficiency. The impeding challenge of demand outstripping

supply for silicon feedstock has lead PV suppliers to move to thinner wafers to save expensive silicon. A major challenge converting to thinner cells is the deterioration of the structural integrity present in thicker cells. Cracked wafers are becoming more common and methods to detect and remove damaged wafers are greatly needed. Whether the solar cells are based on single crystalline or polycrystalline type silicon, similar manufacturing steps lead to the production of complete cells. Many of these steps induce additional stresses on the already weakened wafers including: ingot and brick sawing, chemical etching after depositing thin dielectric or metal films, wafer annealing, soldering of contact strings and lamination of cells into solar panels. Wafer/cell damage in the form of peripheral cracks can be initiated by any of these processes and serves as the starting point for fracture.

To improve the economics of cell manufacturing, the PV industry requires that a special inspection and quality control tool be developed for integration into the production process. This in-line tool will allow us (1) to reject mechanically unstable Si wafers after ingot cutting before they are introduced into further cell processing, (2) to identify wafers with mechanical defects (such as cracks) during production to avoid their in-line breakage and (3) to find cracked cells before they are laminated into modules to avoid panel efficiency reduction and product return from the field. The testing tool must possess the following features at a minimum:

- high speed data acquisition and analysis, matching the approximately 2 s per wafer throughput rate of typical cell lines;
- high stability (reliability and duty cycle) of the hardware performance including wafer loading/unloading and parts movement;
- easy integration into a belt conveyor configuration or cell testing station;
- user-friendly algorithm for wafer/cell rejection with a minimum number of false positives.

Various research groups have presented laboratory results of experimental methods for non-destructive crack detection in Si wafers. The most interesting of them are optical and ultrasonic methods such as optical transmission [1], photoluminescence [2] and electro-luminescence imaging [3], infrared lock-in ultrasound thermography [4] and scanning acoustic microscopy [5]. To our knowledge, none of these techniques completely satisfies all of the specifications listed above for in-line testing and mechanical quality control of Si wafers and solar cells. The optical crack detection system utilizes the transmission of a high intensity flashlight through the wafer and captures the image through optical filters with a CCD camera [1]. Processed wafers with Al backside coating and final solar cells practically inhibit this form of crack detection, unless the crack penetrates the backside contact. This event has a low probability in practice. Additionally, the cracks in Cz-Si wafers can be closed having a width below the optical diffraction limit of $\sim 1 \mu\text{m}$ or not penetrating through the entire thickness of the wafer. This makes them undetectable in the transmission test or through the use of magnifying photography. Luminescence imaging employs the fact that under laser excitation or using forward bias, the Si wafer or solar cell emits infrared light due to band-to-band

electron-hole recombination [2, 3]. These methods rely on cooled CCD cameras to detect the near-infrared part of the emission. Cracks or defects are expected to reduce minority carrier lifetime thereby reducing luminescence efficiency that can be viewed in the images. Though luminescence methods are fast and non-destructive, other types of defects such as surface scratches and dislocations may interfere and mislead crack identification. Additionally, optical detection methods rely on graphic detection and automation that requires fast image recognition software. In [4], the authors proposed using ultrasound vibrations to activate a local heating of the wafers in areas with cracks and image cracks using a near-infrared digital camera. Though this hybrid opto-acoustic approach offers high sensitivity with temperature gradients of tens of degrees, the data acquisition requires minutes due to high lock-in integration time to improve the signal-to-noise ratio. Acoustic analysis using the scanning acoustic microscope (SAM) allows ultrasonic mapping of wafers with accurate identification of cracks at micrometre scale [5]. In SAM, the wafers are placed in a tank with deionized water to couple short nano-second ultrasound pulses with the material. Maps are taken in a raster scan mode over a period of minutes and above. The cracks are visualized through material discontinuity resulting from the acoustic impedance mismatch due to cracks and sharp variation of the reflected acoustic beam intensity and map contrast. The SAM technique is employed in the current paper to support vibration methodology.

Other types of wafer breakage tests rely on mechanical stressing of the wafer. The wafers are tested by stressing them either using an opposing pin support mechanism as in [1] or by passing through rollers [6]. These breakage type tests rely on the fact that micro cracks have been shown to reduce the critical external stress applied to a wafer to cause fracture. Wafers that do not break are considered good and allowed to continue for further processing. These bending or twist tests physically load the wafer to a critical breakage point for undamaged wafers. Another approach uses an optical method which induces stress/strain at predetermined areas of the wafer through concentrated local heating [7]. These types of crack control have evident disadvantages because a critical load is a complicated function of the wafer geometry and crystal type (single versus polycrystalline structure) and have low sensitivity to short mm-length cracks. Solar processing steps (sawing, etching, P-diffusion, antireflection layer coating, contact fringes and back contact deposition) induce numerous manufacturing flaws that can contribute to a lowering or increasing of the critical load. Additionally, loading the wafer can initiate its breakage in areas with high thermo-elastic stress, which is not acceptable.

We reported recently on an alternative approach for crack detection in solar grade Si wafers and cells using the resonance ultrasonic vibrations (RUV) system [8]. The RUV method enables fast and accurate crack detection with simple criteria for wafer rejection from solar cell production lines. The RUV system relies on variation of modal vibration characteristics due to physical variations in the wafers caused by cracks. In Cz-Si wafers it has been shown that increased crack length leads to a decrease in peak frequency and an increase in peak bandwidth. Minimum crack length sensitivity is related to the uniformity of the RUV parameters from wafer

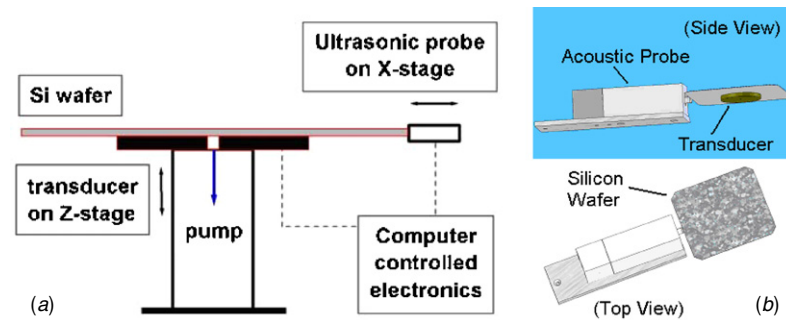


Figure 1. (a) A schematic of the experimental RUV system; (b) mutual layout of the transducer, wafer and probe in the RUV setup.

to wafer within a batch. Typically the RUV system is capable of detecting sub-millimetre length cracks. In this paper we further developed the fundamental aspects of the RUV technique and correlated experimental results on wafers with periphery cracks with finite element analysis (FEA) modelling. FEA provided optimization of crack detection by helping select a proper vibration mode to increase the method sensitivity.

2. Experimental details

Ultrasonic vibrations are induced in an as-cut or processed silicon wafer of symmetrical geometry through a vacuum coupled high frequency piezoelectric transducer beneath the wafer as illustrated in figure 1. Negative pressure applied to the wafer from the vacuum pump modifies the RUV curve, providing peak shifting and broadening due to stress related effects [5], which is observed experimentally at wafer thicknesses under $\sim 100 \mu\text{m}$. This feature can be reduced by appropriate reduction of the negative pressure. Transducer frequency can be swept in the ultrasonic range from 20 kHz to 100 kHz. Standing longitudinal waves are set up at resonance frequencies with peak positions controlled primarily by the wafer's geometry and size, and the material's elastic characteristics. The differing physical attributes of each Si wafer lead to altered resonance mode shapes including peak position, peak bandwidth and peak amplitude. The vibrations are detected using a contact broadband ultrasonic probe pressed against the edge of the wafer under a sensor-controlled force. Stepper motors allow synchronized movement and precise positioning of the wafer and probe for RUV measurements. The entire system is computer controlled and programming devices are operated by Windows-based original software. The RUV unit may be integrated into an automatic belt-type solar cell production line or used as a stand-alone testing system for mechanical quality control.

The transducer beneath the wafer serves as both a holding stage via the vacuum coupling with the wafer as well as serving its primary purpose of inducing resonance vibrations in the form of standing waves in the wafer. The acoustic probe transmits the electrical signal to a computer-controlled lock-in amplifier allowing detection of mV scale ultrasonic signals with sufficient signal-to-noise ratio. In our experiments, the wafer was excited with longitudinal vibrations and a peak resonance of vibrations was detected at specific frequencies

controlled primarily by the wafer's size and material's elastic properties.

When performing RUV experiments with wafers of new sizes or geometries, full spectrum measurements are conducted to locate the exact position of suitable resonance peaks. By exciting the wafers over a wide range of frequencies we can define the natural resonance frequencies. These peaks are characterized by narrow bandwidth, large amplitude and peak separation. Once located further crack analysis is possible on a set of similar wafers. By comparing resonance peak properties, including frequency position, bandwidth and amplitude, of wafers with similar geometries, crystal defects such as cracks or chips can be quickly detected. The RUV method is capable of fast, precise measurements within seconds. The interval includes wafer loading, data acquisition, analyses and wafer unloading. This high speed of measurement makes the RUV system a potential candidate for in-line crack detection matching the throughput rate of the production line. Scanning acoustic microscopy (SAM) was used as a supporting method to visualize cracks with highest resolution of $10 \mu\text{m}$. SAM techniques are described elsewhere [5].

3. Experimental results and modelling

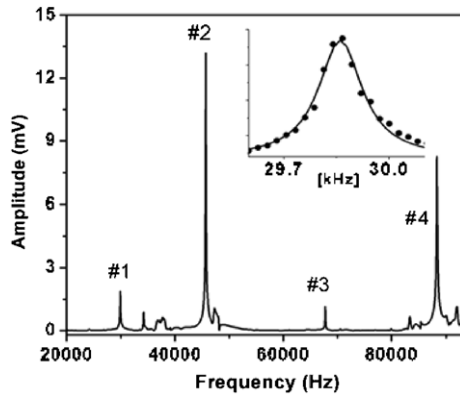
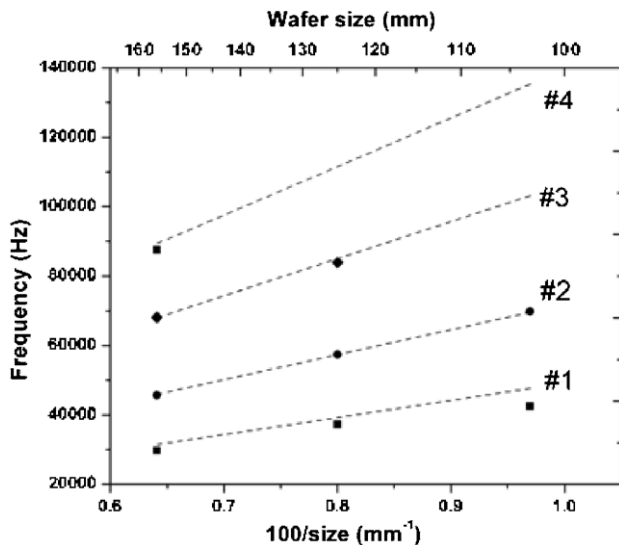
3.1. RUV mode identification

Specific resonance vibration modes were found by first measuring a full spectrum frequency scan on the representative cast and Cz-Si wafers with an illustrative example presented in figure 2 for a $156 \text{ mm} \times 156 \text{ mm}$ cast Si wafer. RUV in square-shaped wafers of different accepted photovoltaic industry standard sizes, and thicknesses ranging from $100 \mu\text{m}$ to over $300 \mu\text{m}$, were measured and their peak positions are summarized in table 1. It is important to note that previous studies have shown minimal RUV parameter shifts with wafer thickness [8]. Each experimental peak represents a particular vibration mode that is compared with FEA results. FEA parameters for analysis include a size specific mesh with square-shaped 1 mm or 2 mm individual elements. The silicon wafer is modelled as an isotropic thin plate with Young's modulus of 167 GPa, a Poisson ratio of 0.3 and a density of $2.3 \times 10^3 \text{ kg m}^{-3}$. Free vibrations of the plate were calculated neglecting the effect of the transducer coupling and acoustic probe contact.

Even in this simplified model, we found a close match of the experimental and calculated frequencies (table 1) in wafers of different sizes. As expected the resonance frequency of a

Table 1. Resonance peak frequencies for four vibration modes in Si wafers of different sizes: (a) experimental data, (b) FEA calculations. Calculated frequencies are rounded to the last digit.

Wafer size (mm)	Peak frequency (kHz)							
	Mode 1		Mode 2		Mode 3		Mode 4	
	(a)	(b)	(a)	(b)	(a)	(b)	(a)	(b)
103 × 103	42.5	47.6	69.8	69.6	–	103.1	–	135.3
125 × 125	37.3	39.3	57.4	57.4	83.8	84.9	–	111.5
156 × 156	29.7	31.5	45.7	45.9	68.2	68.1	87.4	89.3

**Figure 2.** Broad range frequency scan of a 156 mm × 156 mm cast Si wafer. Four individual RUV modes are shown. Insert zooms on the mode 1 at ~30 kHz (points) with Lorentzian fit (solid line).**Figure 3.** Variation of the resonance peak position of four vibration modes presented in figure 2 versus the edge length of the square shaped wafer. Dotted lines: FEA calculations; dots: experimental data on Si wafers.

specific mode (f_{res}) shifts upwards with reducing wafer size (a). It practically obeys a simple relation, such as $f_{res} \sim a^{-1}$ which is illustrated in figure 3 in the case of the four vibration modes numbered in figure 2.

In figures 4(a)–(d) we present FEA mode shapes for resonance vibrations indicated by arrows and numbers in figure 2. Following closely the experimental and

calculated resonance frequencies as seen in table 1 we are confident with this mode identification. To further verify this mode identification and in order to assure that FEA modelling matches the experimental data and provides correct representation of the vibration modes we conducted an experiment to determine the mode shape from a series of amplitude measurements along a wafer's edge. Once the peak vibration frequency of a specific mode was found, the mode shape was analysed by conducting a single peak scan along one edge of the symmetrical wafer noting the amplitude change from point to point that is consistent with peaks and nodes in the modal standing waveform. The resonance peaks were measured with a step size between 3 and 5 mm to construct a representative mode shape. The change in peak amplitude along the edge of the vibrating wafer was found to be similar to the mode shapes at the respective frequency as predicted by FEA. Some asymmetry of the experimental data can be attributed to angular distribution of the transducer's vibrations.

Two unique resonant modes were analysed at approximately 30 kHz and 45.6 kHz, which correspond to peaks 1 and 2 respectively (figure 2) for a 156 mm × 156 mm square shaped cast silicon wafer. Figure 5 demonstrates the correlation between the amplitudes of the experimental data and theoretical FEA results. Experimental edge scans on the other two vibration modes, 3 and 4, also show close relevance to calculated edge scans. Specifically, the number of vibration nodes matches for both modes. However, an accurate fit of the experimental data is complicated due to a larger number of vibration periods for these high-frequency modes and limited spatial resolution of the probe. Good correlation between the experiment and the FEA modelling will serve as a guideline for crack influenced frequency-shifting behaviour.

3.2. RUV crack detection

Due to the fact that finding naturally occurring cracks with the precise position and length necessary for analysis is nearly impossible, cracks were intentionally introduced into the (100) oriented Cz-Si wafer. This was achieved by pressurizing the wafer near the edge at the intended crack location with a diamond tipped scribe. Consistently increasing the pressure until a cracking sound was heard usually achieved the desired results (figure 6).

Because of the possibility for crack propagation in either of two cleavage crystallographic $\langle 110 \rangle$ directions the crack had to be coaxed to propagate in the required direction. This could generally be achieved by scratching (mm-length) the wafer surface along the intended propagation direction and

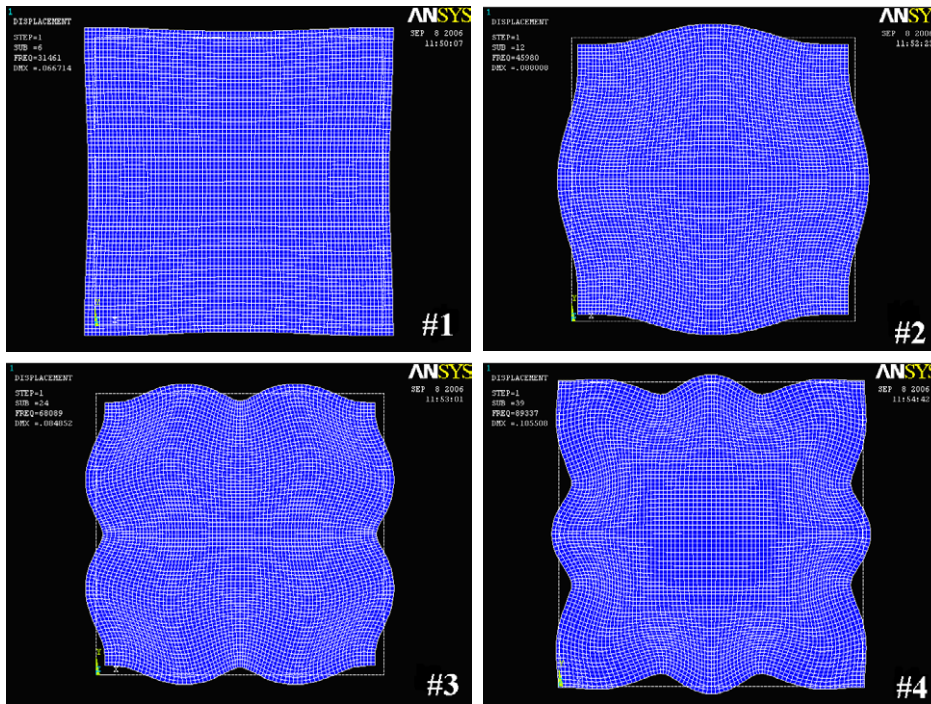


Figure 4. FEA calculated mode shapes corresponding to peaks 1–4 as seen in figure 2.

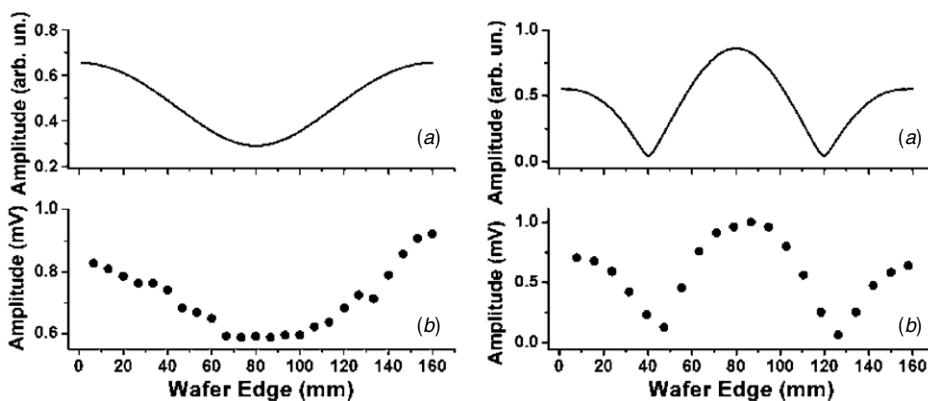


Figure 5. Amplitude variation of the RUV mode along the wafer edge representing peak 1 at 30 kHz (left) and peak 2 at 45.6 kHz (right). (a) FEA modelling, (b) experimental data.

then pressurizing the wafer edge with the diamond scribe. Crack making without initial directional forcing damage was often used due to its ease and lack of extra wafer damage from scribing. Cracks typically appeared as singular cracks in either ‘left’ or ‘right’ crystal directions or as dual cracks heading in both directions simultaneously from the point of pressure. Crack elongation can be achieved by finding the tip of the initial crack and slightly pressurizing it with the diamond scribe, which can lead to crack ‘branching’ as illustrated in figure 6(c). To avoid this undesirable effect a consistent crack elongation without ‘branching’ cracks can be achieved by precise pressurizing at the crack tip as seen in figures 6(d) and (e).

We performed an RUV experiment on a set of identical in size 125 mm × 125 mm production grade cast wafers with the results presented in figure 7. This sequential RUV data collection and analysis is closely relevant to the solar

cell testing routine targeting to reject mechanically unstable Si wafers in PV production. Three parameters of the RUV peak were analysed: peak position, peak bandwidth and peak amplitude. One of the wafers (11) was clearly an outlier inconsistent with the other wafers. Using SAM measurements we confirmed that this wafer had a 10 mm periphery crack which was clearly observed in the RUV testing.

The following experiments were carried out using Cz–Si wafers to determine the sensitivity of the RUV system to cracks originating from the edge centre versus corner position. It can be seen in figure 8 that in the centre crack position the peak 2 mode is less sensitive to the 6 mm crack and shows a small downward frequency shift of 18 Hz, negligible bandwidth broadening and only a slight reduction in amplitude (0.2 mV). In comparison, the peak 3 mode shows a substantial downward frequency shift of 655 Hz along with the amplitude reduction of 1.7 mV and bandwidth increasing by 40 Hz for the same

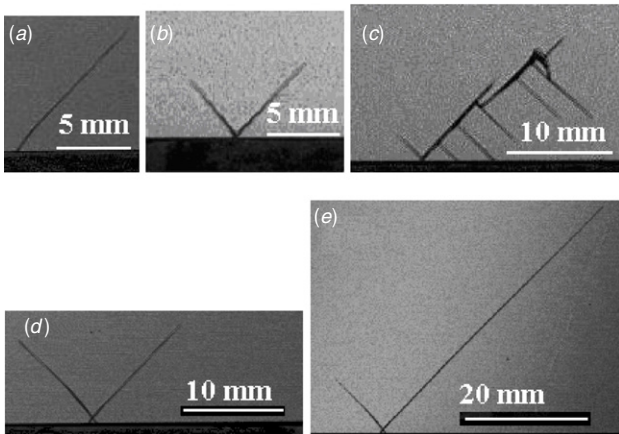


Figure 6. SAM images present possible crack propagation orientations: (a) single, (b) dual, (c) incorrectly formed branched crack, (d) wafer with initial induced crack and (e) the same wafer after successful elongation.

wafer and same crack. In contrast to this, the corner crack is more prominent in the variation of mode 2 versus mode 3, as illustrated in figure 9. Through the use of FEA analysis we have been able to understand the apparent selective sensitivity of certain RUV modes to peripheral cracks.

These experimental data were compared with FEA analyses using the algorithm described in [5]. The model crack was located at the wafer centre or at the corner at 45° with respect to the wafer edge, similar to the experiment. The crack length was changed from 1 mm to 16 mm and peak position was calculated for vibration mode numbers 1, 2 and 3 in figure 2 with resonance frequencies at 40, 58 and 86 kHz (according to a size scaling factor). The results presented in figure 10 illustrate that in the case of a central crack, the shift of mode 3 is the largest while for the corner crack it is opposite, which is consistent with the experimental data in figures 8 and 9.

This interesting feature can further improve crack detection sensitivity by tracking the RUV parameters of different vibration modes to minimize the probability of passing a cracked wafer through the production line.

The RUV technique has proven to be a viable candidate for in-line crack detection in industry standard size and thickness

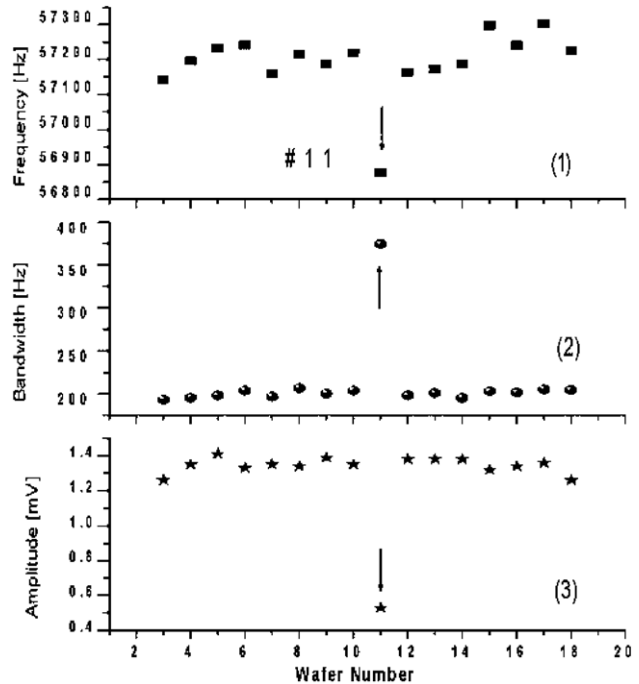


Figure 7. Crack detection run on a set of $125 \text{ mm} \times 125 \text{ mm}$ cast wafers, monitoring peak 2, with wafer 11 possessing a 10 mm periphery crack identified by RUV parameter variations: (1) peak position, (2) peak bandwidth and (3) peak amplitude.

silicon wafers for solar cells. Experiments, such as the one in figure 7, have shown the RUV technique capable of picking out cracked wafers by monitoring their resonance peak characteristics including peak amplitude, bandwidth and frequency. In an effort to increase the system's sensitivity we used FEA modelling to identify vibration modes in the range from 20 kHz to 100 kHz and through physical experimentation found that certain modes are more sensitive to cracks at specific positions. By monitoring more than one mode, cracks at virtually any position in the wafer can be detected. The RUV technique holds promise, with further advancements in sensitivity, accuracy and speed necessary, as a valuable quality control tool for the photovoltaic industry.

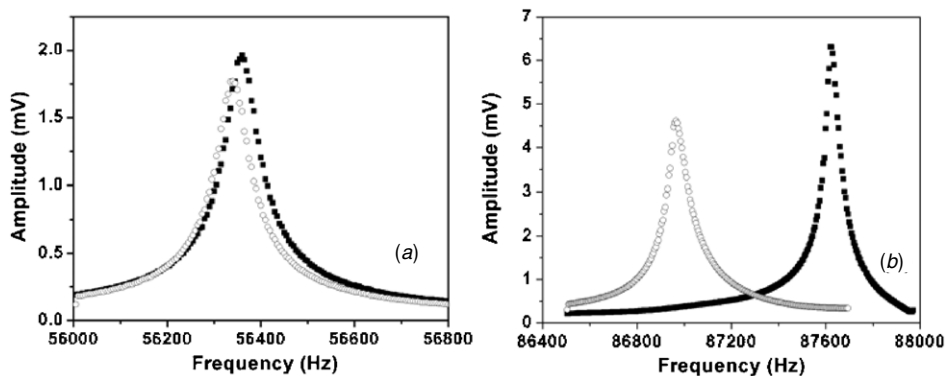


Figure 8. (a) Peak 2 mode showing a small RUV parameter shift when a 6 mm crack was introduced into the wafer's edge at the centre. (b) Peak 3 mode showing larger RUV parameter variation on the same cracked wafer. Closed squares represent the undamaged wafer, open circles represent the cracked wafer.

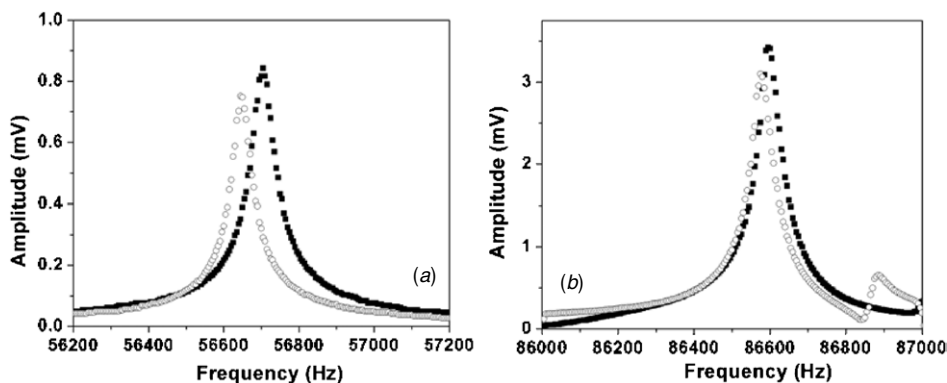


Figure 9. Peak 2 mode (a) showing a larger RUV parameter shift compared to peak 3 (b) when a 3 mm crack was introduced into the wafer's corner.

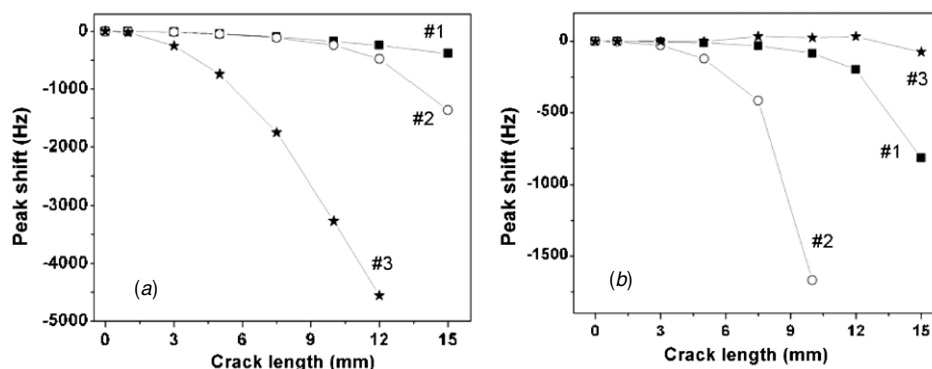


Figure 10. (a) FEA calculated variation of the peak position versus crack length for a centre crack position for vibration modes 1, 2 and 3; (b) same for a crack at the corner position.

Acknowledgments

The work was supported by the NREL sub-contract AAT-2-31605-6 and NSF award DMI-0523163.

References

- [1] Rueland E, Herguth A, Trummer A, Wansleben S and Fath P 2005 Optical u-crack detection in combination with stability testing for in-line inspection of wafers and cells *Proc. 20th EU PVSEC (Barcelona)* pp 3242–5
- [2] Trupke T, Bardos R A, Schubert M C and Warta W 2007 Photoluminescence imaging of silicon wafers *Appl. Phys. Lett.* **89** 044107
- [3] Fuyuki T, Kondo H, Yamazaki T, Takahashi Y and Uraoka Y 2005 Photographic surveying of minority carrier diffusion length in polycrystalline silicon cells by electroluminescence *Appl. Phys. Lett.* **86** 262108
- [4] Rakotoniaina J P, Breitenstein O, Al Rifai M H, Franke D and Schnieder A 2004 Detection of cracks in silicon wafers and solar cells by lock-in ultrasound thermography *Proc. PV Solar Conf. (Paris, June)* pp 640–3
- [5] Belyaev A, Polupan O, Ostapenko O, Hess D and Kalejs J P 2006 Resonance ultrasonic vibration diagnostics of elastic stress in full-size silicon wafers *Semicond. Sci. Technol.* **21** 2540260
- [6] Behnken H, Apel M and Franke D 2003 Simulation of mechanical stress during bending tests for crystalline wafers *3rd World Conf. on Photovoltaic Energy Conversion (Japan)*
- [7] Sopori B, Sheldon P and Rupnowski P 2006 Wafer breakage mechanism(s) and a method for screening 'problem wafers' *16th Workshop on Crystalline Silicon Solar Cells and Modules (Denver, CO)*
- [8] Belyaev A, Polupan O, Dallas W, Ostapenko S, Hess D and Wohlgenuth J 2006 Crack detection and analyses using resonance ultrasonic vibrations in full-size crystalline silicon wafers *Appl. Phys. Lett.* **88** 111907